Journal of Hazardous Materials 189 (2011) 420–426

Contents lists available at ScienceDirect

Journal of Hazardous Materials

journal homepage: www.elsevier.com/locate/jhazmat

Characteristics of cellulosic amine-crosslinked copolymer and its sorption properties for Cr(VI) from aqueous solutions

Xing Xu, Bao-Yu Gao*, Xin Tang, Qin-Yan Yue, Qian-Qian Zhong, Qian Li

Key Laboratory of Water Pollution Control and Recycling (Shandong), School of Environmental Science and Engineering, Shandong University, Jinan 250100, PR China

ARTICLE INFO

Article history:
Received 15 December 2010
Received in revised form 14 February 2011
Accepted 16 February 2011
Available online 23 February 2011

Keywords:
Cotton stalk peel
Amination
Cr(VI)
Desorption
Raman spectrum

ABSTRACT

A new cellulosic amine-crosslinked copolymer was prepared after the amination reaction with cotton stalk peel (CSP). The physicochemical characteristics of amine-crosslinked cotton stalk peel (AC-CSP) and raw CSP were determined after the surface analysis (including specific surface area, micropore volume and SEM), zeta potential analysis and spectrum analysis (FTIR and Raman spectrum). The sorption properties of AC-CSP for Cr(VI) were evaluated in the static, column sorption and desorption tests. The surface characteristics indicated the absence of porous adsorption in the potential Cr(VI) sorption mechanism. Zeta potential and spectrum analysis of AC-CSP illustrated the involvement of amine groups in the Cr(VI) sorption process. The sorption capacity of AC-CSP for Cr(VI) was 129.0 mg/g as comparison with 14.8 mg/g of raw CSP. Flow rate and influent Cr(VI) concentration were demonstrated as two influencial factors in the column sorption tests. NaCl was used as the eluent, and the desorption efficiencies during three successive cycles were 75.9%, 69.8% and 64.3%, respectively. In addition, the results of the static, column sorption and desorption tests illustrated the complicated interactions between Cr(VI) and AC-CSP including complexation and ion exchange mechanisms.

1. Introduction

Chromium is primarily present in the form of hexavalent Cr(VI) as chromate (CrO_4^{2-}) and dichromate ($Cr_2O_7^{2-}$). Cr(VI) is largely employed in the chemical industry for battery, textiles, rubbers, electroplating, leather tanning, wood preservations, manufacturing of dye, paint, paper, and petroleum refining processes [1,2]. The effluents from these industries contain Cr(VI) in concentrations ranging from tens to hundreds of milligrams per litre. While potable waters containing more than 0.05 mg/L chromium are considered to be toxic and result in human diseases including skin irritation to lung cancer, as well as kidney, liver, and gastric damage [3]. In this way, Cr(VI) must be removed from industrial effluents before being delivered into the environment. The common procedures for Cr(VI) removal from industrial effluents include ion-exchange resins, chemical precipitation, organic groups grafted on textiles and separation by specific membranes [4]. Biosorption, an alternative process, is competitive and cheap. Biosorption is a term that usually describes the removal of heavy metals from aqueous solutions through passive binding to the surface of biomaterials. Various naturally available biomaterials like pistachio hull [5], green algae [6], sawdust [7], seaweed [8], peanut shell [9], lichen [10] and coconut shell [11] were used for the removal of chromium Cr(VI). However, many of these naturally available biomaterials have low Cr(VI) adsorption capacities and slow process kinetics. Thus, a further chemical modification on these biomaterials would be required to increase their potential adsorption capacities for Cr(VI).

In recent years, more and more attentions have been focused on the modified biomaterials and numerous studies have shown their excellent sorption capacities for various metal ions [11–13]. The availability of the chemical process (e.g., esterification, etherification and copolymerization) on biomaterials modification could be attributed to the particular properties of biomaterials such as chemical stability and high reactivity, resulting from the presence of reactive hydroxyl groups in cellulose chains [10,14–16].

In this work, a new kind of biosorbent was prepared from cotton stalk peel (CSP) by amination reaction, which produced the cellulosic amine-crosslinked copolymer. The high content of cellulose in cotton stalk peel favored the amination process, and could greatly enhance the efficiency of grafting. The physicochemical and sorption properties of amine-crosslinked cotton stalk peel (AC-CSP) were measured by zeta potential, BET, FTIR, SEM and Raman spectrum techniques. Sorption properties of AC-CSP in static tests were studied by varying the conditions such as initial pH, contact time and temperature. In addition, sorption characteristics of AC-CSP in fixed-bed column were studied by varying the influent conditions in the continuous system such as influent Cr(VI) concentrations

* Corresponding author. Tel.: +86 531 88364832; fax: +86 531 88364513.
E-mail addresses: bygao@sdu.edu.cn, baoyugao_sdu@yahoo.com.cn (B.-Y. Gao).

0304-3894/$ – see front matter © 2011 Elsevier B.V. All rights reserved.
doi:10.1016/j.jhazmat.2011.02.056

and flow rates. What is more, desorption and dynamic elution tests were repeated in fixed-bed column for several sorption–desorption cycles and the regeneration property of AC-CSP was evaluated by using NaCl as the desorption eluent.

2. Materials and methods

2.1. Preparation of the AC-CSP

CSP was obtained from Binzhou, Shandong, China. The raw CSP was washed with water, dried at 60 °C for 12 h and sieved into particles with diameters from 0.5 to 2.0 mm.

Ten gram of CSP was reacted with 4.5 ml of epichlorohydrin and 2.0 ml of N,N-dimethylformamide in a three-neck round bottom flask at 85 °C for 60 min, followed by adding 1.5 ml of ethylenediamine and the mixture was stirred for 90 min at 85 °C. The product was washed with 150 ml of distilled water to remove the residual chemicals, dried at 60 °C for 12 h and sieved to obtain particles smaller than 1.0 mm in diameter [14,17,18]. The scheme of the reaction is shown in Fig. 1.

2.2. Characteristics of raw CSP and AC-CSP

2.2.1. Surface characteristics analysis

Analysis of surface characteristics of the raw CSP and AC-CSP included BET specific surface area, micropore volume, pore size distributions and SEM observation. A photomicrography of exterior raw CSP and AC-CSP surface was obtained by SEM (Hitachi-S-2400, Japan). Other characteristics including specific surface area, micropore volume and pore size distributions were determined by the nitrogen adsorption isotherm technique, with an automatic BET surface area analyzer (Model F-Sorb 2400, Beijing Jinaipu Technical Apparatus Co., Ltd., China). The nitrogen adsorption was carried out at 77 K.

2.2.2. Zeta potential analysis

A microelectrophoresis apparatus (JS94H, Shanghai Zhongchen Digital Technical Apparatus Co., Ltd., China) was used to determine the zeta potentials of raw CSP and AC-CSP. The raw CSP or AC-CSP sample was prepared in 25 ml of distilled water containing 0.1 g of raw CSP or AC-CSP. In addition, the Cr(VI)-loaded AC-CSP sample was prepared by comprising the suspensions with 0.1 g of AC-CSP and 100 mg/L Cr(VI).

2.2.3. Spectrum analysis

FTIR and Raman spectroscopic analysis was performed to provide insights into the structure change between raw CSP and AC-CSP as well as the mechanisms of Cr(VI) interactions with AC-CSP.

The functional groups presenting in raw CSP and AC-CSP were investigated by using the FTIR technique (Perkin–Elmer "Spectrum BX" spectrometer). The spectrum was scanned from 400 to 4000 cm^{-1}. In the Raman analysis, 0.1 g AC-CSP was placed in 50 ml of potassium dichromate solution with concentration of 0.5 mol/L. The wet solid samples and potassium dichromate solution (1 mol/L) were analyzed by Raman spectroscopy (Nicolet Almega XR Dispersive Raman, Thermo Electron Corporation, USA). The laser wavelength used in Raman measurement was 1050 nm.

2.3. Sorption tests

2.3.1. Static sorption tests

The static sorption tests were carried out by using a sample containing 0.1 g of AC-CSP and 50 ml of Cr(VI) solution in 250 ml flasks and shaking on a horizontal shaker. The initial pH value of the solution, which was 5.12, was used throughout all sorption experiments. In the contact time test, at specified time intervals of 1, 3, 5, 10, 15, 30, 60, 120, 180 and 240 min, an aliquot of sample was taken and analyzed for the residual concentration of Cr(VI) in the supernatant solution. In the pH tests, initial pH values were designed in the range of 2.0–8.0 and the pH was adjusted using 0.1 mol/L of HCl and NaOH. In the batch equilibrium experiments, the sorption experiments were performed at various initial concentrations for 240 min at three temperatures (293, 303 and 313 K), respectively. The concentration of the output solution was measured using UV-vis spectrophotometer, and all the experiments were performed in duplicate and the average result was taken for calculation.

Table 1
Surface characteristics of raw CSP and AC-CSP.

Biosorbent	Specific surface area (m^2/g)	Micropore volume (cm^3/g)	Pore width (nm)
Raw CSP	8.824	0.947	1.688
AC-CSP	6.216	0.739	1.235

2.3.2. Fixed-bed column sorption and desorption tests

Column studies (Up flow mode) were conducted in organic-glass column with an internal diameter of 1.2 cm and 20 cm in length packed with 1.0 g of AC-CSP (bed height: 2.0 cm). The flow rates were controlled at about 3.3, 5 and 10 ml/min and the concentrations of Cr(VI) solutions were 200, 300 and 500 mg/L. The effluent solutions were collected, and every 10 ml was selected as a sample to determine the concentrations of Cr(VI) in the effluent solutions. The flow to the column was continued until the effluent Cr(VI) concentration (C_t) approached the influent concentration (C_0), $C_t/C_0 = 0.98$.

Operation of the column was stopped when the effluent Cr(VI) concentration reached a constant value. Afterwards, the Cr(VI)-loaded biosorbent was regenerated by eluting the distilled water or sodium chloride (NaCl) solution through the exhausted column. The sorption–desorption cycles were repeated for three times and the regeneration capacity for each cycle was calculated.

3. Results and discussion

3.1. Characteristics of raw CSP and AC-CSP

3.1.1. Surface characteristics analysis

The specific surface area, micropore volume and pore size distributions of raw CSP and AC-CSP are shown in Table 1. The specific surface area of the raw CSP is about 8.824 m^2/g, which is slightly higher than that of AC-CSP (6.216 m^2/g). The decrease in the specific surface area of AC-CSP may be attributed to the grafting of the chemical reagents on the surface of raw CSP, which leads to a constriction of the pore channels existing in the internal framework of AC-CSP. This result is validated by the decreased micropore volume in AC-CSP (0.739 cm^3/g) as compared with raw CSP of 0.947 cm^3/g.

The results of the SEM measurements for the surface of raw CSP and AC-CSP are shown in Fig. 2. It is obvious that the surface of AC-CSP is smoother than that of raw CSP; this indicates that the order of cellulose has been improved after the removal of extractives during the amination reaction [18,19]. In addition, the smooth surface of AC-CSP illustrates the absence of porous structure in AC-CSP, which indicates that porous adsorption could be negligible in the potential Cr(VI) sorption mechanism.

3.1.2. Zeta potential analysis

Sorption of Cr(VI) onto AC-CSP is a process of considerable complexity and it is an interesting challenge in understanding the Cr(VI) solution and interfacial behavior of suspensions. Therefore, it is

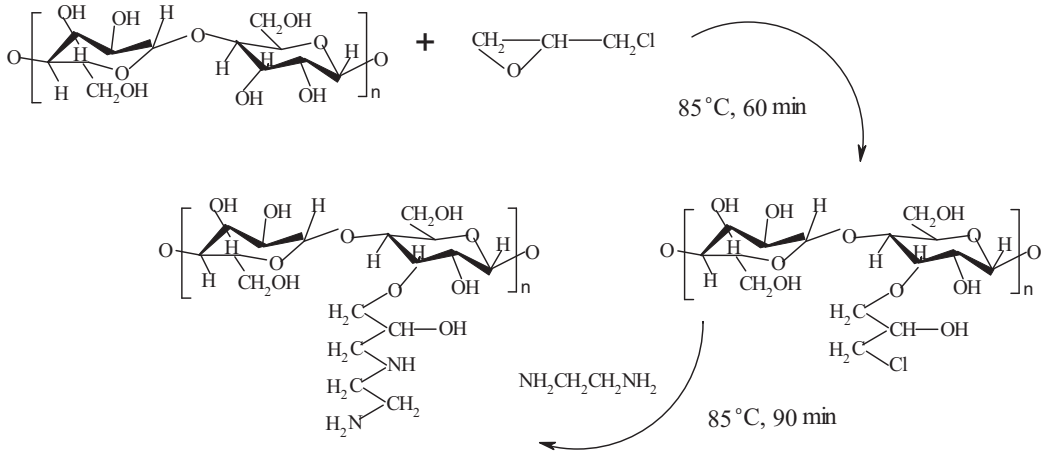

Fig. 1. Scheme of the amination reaction for AC-CSP.

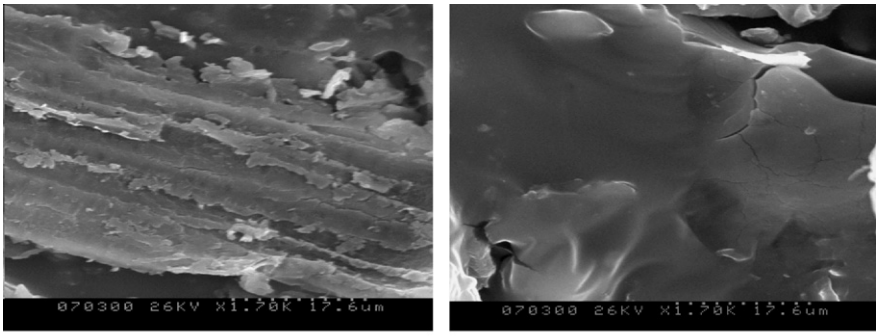

Fig. 2. SEM of raw CSP and AC-CSP.

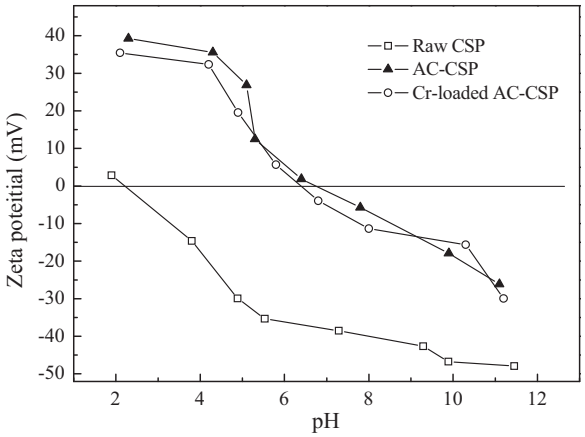

Fig. 3. Zeta potentials of raw CSP, AC-CSP and Cr(VI)-loaded AC-CSP as a function of pH.

necessary to investigate the electrokinetic properties of the suspensions in distilled water and Cr(VI) solution.

Zeta potentials of raw CSP and AC-CSP in distilled water as a function of pH are shown in Fig. 3. The zeta potentials of raw CSP samples decrease from +2.2 mV to −46.3 mV as the initial pH of the suspensions increases from 2.0 to 12.0. For a biomaterial containing cellulose and hemicellulose, reducing solution pH would cause the hydroxyl and carboxyl groups to be protonated and make the surface become positive to an extent [20]. These groups can be deprotonated at basic condition, resulting in the decrease in the zeta potential. In contrast with the raw CSP samples, the zeta potentials of AC-CSP are in the range of −26.4 to +39.3 mV in designed pH range; this indicates the existence of increased positive-charge functional groups on the framework of AC-CSP.

Fig. 3 also shows the zeta potentials of AC-CSP in Cr(VI) solution. The values of positive charges on the surface of Cr(VI)-loaded AC-CSP decrease as comparison with those of AC-CSP in distilled water. This result was consistent with the observation of Yoon, which could be attributed to the steric effects resulting from the displacement of chloride ions by the adsorbed ions [21].

3.1.3. Spectrum analysis

Fig. 4a shows the FTIR spectra of raw CSP and AC-CSP. In contrast with the raw CSP, an obvious new absorption peak at 1325 cm^{-1} is observed in the spectra of AC-CSP, which was assigned to the stretching vibration of C–N in the base of amine groups [22]. The band at 1415 cm^{-1} corresponds to –NH deformation vibration in $–NH_2$. This indicates that ethylenediamine has reacted with cotton cellulose to form cellulosic amine-crosslinked copolymer. In addition, the relative absorbance of hydroxyl bands in spectra of AC-CSP at 3420 cm^{-1} (primary –OH) decreases as comparison with that of raw CSP. This can be attributed to the reaction of chemical reagents with hydroxyl groups on the cellulose chains [23,24].

The Raman spectra of Cr(VI) solutions, AC-CSP and Cr(VI)-loaded AC-CSP are shown in Fig. 4b. The arising of bands at 2968.6, 1612.5 and 1456.6 cm^{-1} corresponds to characteristic peaks of cellulose chains in AC-CSP. Cr(VI) ion in a 0.5 mol/L of potassium dichromate solution has a characteristic peak at 903.3 cm^{-1}. It is observed that the characteristic peak of Cr(VI) solution (903.3 cm^{-1}) is significantly shifted to a new peak (839.9 cm^{-1}) after the sorption of Cr(VI) onto AC-CSP. This indicates that the bonding environment

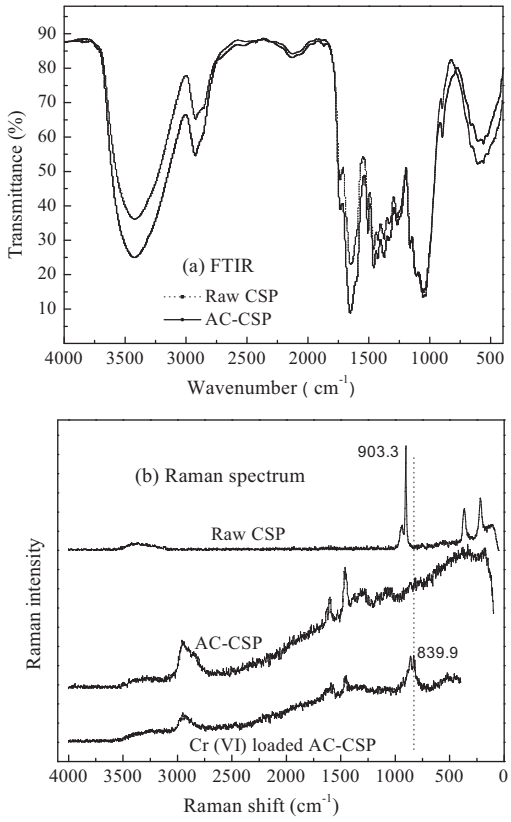

Fig. 4. Spectrum analysis of raw CSP and AC-CSP (a) FTIR spectrum; (b) Raman spectrum.

between Cr(VI) and AC-CSP is quite different from that of free Cr(VI) ions in the solution. As suggested by Yoon, this significant shift of peaks between different forms of Cr(VI) indicates the complicated interactions between Cr(VI) ions and AC-CSP [21].

FTIR and Raman spectrum analysis illustrate a potential relationship between the Cr(VI) sorption mechanisms and the functional groups in AC-CSP. In order to understand the detailed interactions between Cr(VI) ions and AC-CSP, sorption properties of Cr(VI) onto AC-CSP would be discussed in the static, column sorption and desorption tests.

3.2. Static sorption tests

3.2.1. pH

The sorption of Cr(VI) onto raw CSP and AC-CSP as a function of pH are shown in Fig. 5. Equilibrium pH values were examined after the uptake of Cr(VI) by raw CSP and AC-CSP at different initial pH. A significant decrease in the equilibrium pH is observed as compared to the initial pH values with range of 6.0–8.0. This could be attributed to the weakly acidic hydroxyl and carboxyl inherently in raw CSP and AC-CSP, which would decrease the pH of solutions in mild alkali conditions [25].

It is observed in Fig. 5 that initial uptake of Cr(VI) increases with an increase of pH from 2.0 to 3.0 thereafter uptake decreases with the increase of pH from 3.0 to 8.0. Cr(VI) exists in the form of oxyanions in aqueous solution such as $HCrO_4^-$, $Cr_2O_7^{2-}$ and CrO_4^{2-} ions, among which the $HCrO_4^-$ ion is stable and dominant at pH values lower than 5.0 [26]. In acidic medium, the lowering of pH causes the amine active sites in AC-CSP to be protonated and as a result a strong attraction exists between Cr(VI) ions and amine groups. Hence, the uptake increases with the decrease in the pH of the solution. Whereas at high pH, biosorbent surface will be negatively charged and in addition to this there will be competition between

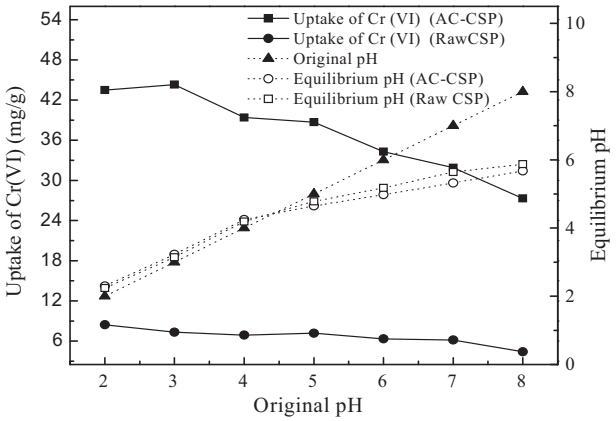

Fig. 5. Sorption of Cr(VI) onto raw CSP and AC-CSP as a function of pH (Cr(VI) concentration: 200 mg/L, contact time: 180 min, dosage: 2 g/L, temperatures: 20 °C).

OH– and Cr(VI) ions. Both these factors cause hindrance in the sorption of negatively charged Cr(VI) ions, etc. resulting in the decreased uptake of Cr(VI) at high pH value. The mechanism of interaction of Cr(VI) ion ($HCrO_4^-$) with AC-CSP can be represented as follows:

$$RNH_2{}^+Cl^- + HCrO_4^- \leftrightarrow RNH_2{}^+HCrO_4^- + Cl^- \quad (1)$$

Fig. 5 also shows the uptake of Cr(VI) by raw CSP. The Cr(VI) sorption capacity of raw CSP at pH 2.0–3.0 is about 7–8 mg/g. At acidic pH 2.0–3.0, the hydroxyl and carboxyl groups in raw CSP might be highly protonated which results in the binding of anionic Cr(VI) ion species onto the positively-charged surface of raw CSP. As reported by Wang et al. [27], many natural biomaterials including sugarcane bagasse (13.5 mg/g), almond shell (21.8 mg/g) and ground nut shell (29.6 mg/g) have shown the sorption capacities for Cr(VI). The binding of the Cr(VI) ions with natural biomaterials may be attributed to the partial conversion of Cr(VI) to the reduced form of Cr(III) on the surface of the biomaterials [28–30]. It consists of three steps [30]: (i) the binding of anionic ($HCrO_4^-$) Cr(VI) to the positively-charged groups present on the surface of the biomaterials at pH 2.0–3.0 (Eq. (2)), (ii) the reduction of adsorbed Cr(VI) into Cr(III) by adjacent electron-donor (C=O, O–CH_3) groups (Eq. (3)) and (iii) the complexation of the reduced-Cr(III) with adjacent groups, i.e., Cr-binding groups (Eq. (4)). Carboxyl groups in biomaterials are suspected to bind anionic Cr(VI) ions with the aid of protons in aqueous phase:

$$B\text{–}COOH + HCrO_4^- + H^+ \rightarrow B\text{–}COOH_2{}^+\cdots HCrO_4^- \quad (2)$$

$$B^+\cdots HCrO_4^- + H^+ \rightarrow B\text{–oxidized groups} + Cr^{3+} + H_2O \quad (3)$$

$$B\text{–}3(COOH) + Cr^{3+} \rightarrow B\text{–}3(COO^-)\cdots Cr^{3+} + 3H^+ \quad (4)$$

This complex interaction with the chemical binding groups should also exist in the sorption of Cr(VI) by AC-CSP. And therefore, it is suggested that the sorption mechanisms for Cr(VI) onto AC-CSP could be related to the complicated interactions including complexation, electrostatic attraction and so forth.

3.2.2. Contact time

The effect of contact time on the sorption of Cr(VI) by AC-CSP at different initial concentrations (30, 50 and 80 mg/L) is represented in Fig. 6. These experimental data were recorded at constant pH (pH 5.12) and the equilibrium time was measured at 240 min to make sure that full equilibrium was attained. The sorption process shows a rapid increase during the first 30 min for all concentrations. Thereafter the rate of sorption is found to be slow and finally approaches equilibrium. For 30 mg/L Cr(VI), 14.7 mg Cr(VI)/g AC-CSP is adsorbed after equilibrating for only 25 min. But for 50 mg/L Cr(VI), 23.1 mg/g is adsorbed after 60 min and for 80 mg/L Cr(VI), a

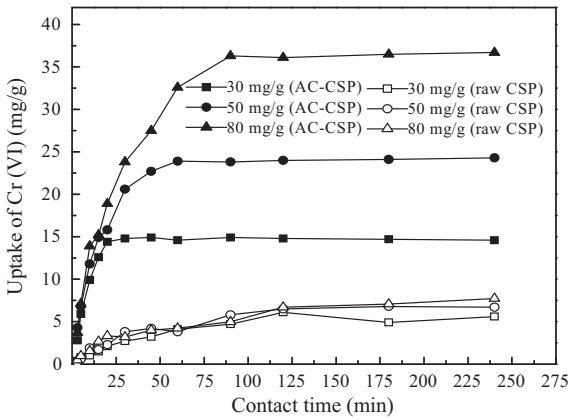

Fig. 6. Effect of contact time on the sorption of Cr(VI) by raw CSP and AC-CSP (Cr(VI) solution pH: 5.12, dosage: 2 g/L, temperatures: 20 °C).

maximum of 35.7 mg/g is adsorbed after equilibrating for 90 min. It is evident that an increase in the initial Cr(VI) concentration leads to a notable increase in the equilibrium time and sorption amount. However, the removal percent of Cr(VI) decreases from 99.0% to 89.3% as Cr(VI) initial concentrations increases from 30 to 80 mg/L. Therefore, the sorption of Cr(VI) by AC-CSP has a strong dependence on the initial concentration.

Similar results are also shown in the sorption of Cr(VI) by raw CSP, and the Cr(VI) sorption capacity of raw CSP at equilibrium is found to be 5.6, 6.7 and 7.2 mg/g at initial concentrations of 30, 50 and 80 mg/L, respectively.

3.2.3. Adsorption isotherms

Adsorption isotherms can be used to describe how solutes interact with the adsorbent and therefore it is critical in optimizing the use of the adsorbent. Isotherm studies provide information on the capacity of adsorbent, which is the most important parameter for a sorption system. In this study, equilibrium data of raw CSP and AC-CSP at various temperatures (20, 30, 40 °C) were analyzed by two empirical adsorption models, namely Langmuir and Freundlich isotherms. These isotherms relate Cr(VI) uptake per unit weight of biosorbent (raw CSP or AC-CSP) q_e to the equilibrium Cr(VI) concentration in the bulk fluid phase C_e.Langmuir equation [18]:

$$\frac{1}{q_e} = \frac{1}{q_{max}} + \left(\frac{1}{q_{max} K_L}\right)\frac{1}{C_e} \quad (5)$$

Freundlich equation [18]:

$$\ln\ q_e = \ln\ K_F + \frac{1}{n}\ln\ C_e \quad (6)$$

where C_e, the equilibrium dye concentration in solution (mg/L); q_{max}, the monolayer capacity of the sorbent (mg/g); K_L, the Langmuir constant (L/mol); K_F, the Freundlich constant (L/g).

The theoretical parameters of isotherms along with regression coefficient are listed in Table 2 (figure was not list). The Langmuir isotherm model has higher regression coefficient when compared to Freundlich model, indicating the homogeneous nature of raw CSP and AC-CSP. Increase in Langmuir constant K_L and q_{max} with temperature confirms the endothermic nature of adsorption and Freundlich constant K shows the favorability of adsorption at higher temperatures [31].

Table 3
Comparison of sorption capacity for Cr(VI) with various adsorbents.

Adsorbent	Maximum uptake capacity (q_{max}) (mg/g)	References
Wheat bran	40.8	[32]
Rice bran	58.9	[32]
P. yezoensis Ueda (red algae)	56.3	[32]
Padina (brown algae)	54.6	[33]
Tyres activated carbon	58.5	[34]
Activated weed	247.0	[13]
Sawdust activated carbon	44.05	[35]
Amberlite IRA-900	149.9	[36]
Raw CSP	13.8	This study
AC-CSP	129.0	This study

A comparison of the sorption capacities for Cr(VI) by other low-cost biosorbents is given in Table 3. The high sorption capacity of this study reveals that AC-CSP could be a promising biosorbent for Cr(VI) removal.

3.3. Column sorption tests

When the sorption zone moves up and the upper edge of this zone reaches the bottom of the column, the effluent concentration starts to rise rapidly. This is called the breakthrough point. The desired breakthrough point was determined to be 0.1 C_t/C_0. The point where the effluent concentration reached 95% ($C_t/C_0 = 0.95$) of its influent value is called the point of column exhaustion.

3.3.1. Comparison of raw CSP and AC-CSP in the column sorption test

The raw CSP's column sorption capacity for Cr(VI) ion is about 12.5 mg/g, and results shown in Fig. 7 indicate that the Cr(VI) sorption capacity of AC-CSP (95.6 mg/g) has been greatly enhanced in contrast with that of raw CSP. As is shown in Fig. 7, the breakthrough points of raw CSP and AC-CSP occur at the breakthrough volumes of 30 and 350 ml, respectively. As the Cr(VI) solution continues to flow into the column, the two biosorbents gradually become saturated with Cr(VI) ions and become less effective for further sorption. The points on the S-shaped curves of raw CSP and AC-CSP at which the Cr(VI) concentrations approach their exhaustion values are about 180 and 660 ml, respectively.

3.3.2. Effect of flow rate on the sorption of Cr(VI) by AC-CSP

Flow rate is one of the important characteristics in evaluating adsorbents for continuous treatment of metal laden effluents. To find out the effect of flow rate on breakthrough curve, sorption experiments were carried out by varying the flow rates between 3.3 and 10 ml/min. In this process, the initial concentrations, ini-

Table 2
Parameters in Langmuir and Freundlich models.

	T (°C)	Langmuir			Freundlich		
		q_{max} (mg/g)	K_L	R^2	K	n	R^2
AC-CSP	20	117.9	0.024	0.9833	0.36	3.74	0.926
	30	121.9	0.025	0.9971	11.8	2.72	0.989
	40	129.0	0.028	0.9895	13.0	2.72	0.961
Raw CSP	20	13.8	0.014	0.9788	2.9	2.99	0.896
	30	14.2	0.016	0.9856	13.8	2.87	0.945
	40	14.8	0.017	0.9915	14.0	2.79	0.957

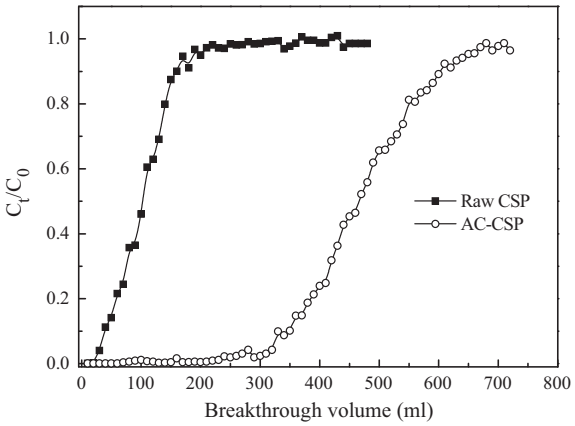

Fig. 7. Sorption capacity of Cr(VI) by raw CSP and AC-CSP (influent Cr(VI) concentration: 200 mg/L, influent pH: 5.12; flow rate: 3.3 ml/min; bed height: 2.0 cm).

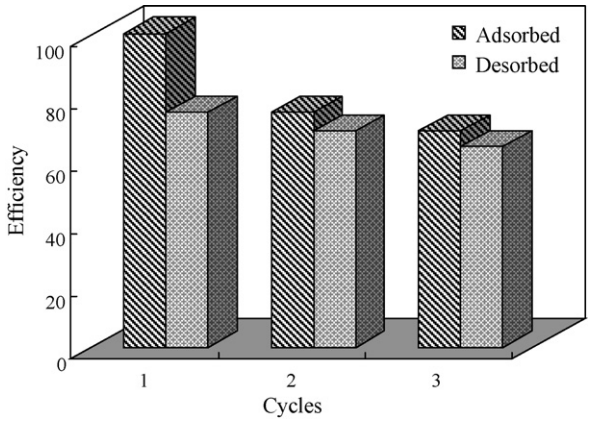

Fig. 9. Sorption–desorption cycles for AC-CSP (elution rate: 3.3 ml/min, NaCl concentration: 1 mol/L).

tial influent pH and bed height were maintained at 200 mg/L, 5.12 and 2.0 cm, respectively. The effect of flow rate on breakthrough performance at the above operating conditions is shown in Fig. 8b. It can be seen from the figure that the sorption capacity is higher at lower flow rate. As shown in some literatures, the sorption of some metal ions in fixed-bed column often displayed a general trend of increase with decrease in flow rate; this may be attributed to an increase in residence time which results in the more time to bond with the metal efficiently [7,36,37]. The breakthrough volume decreases from 350 to 260 ml as the flow rate increases from 3.3 to 10 ml/min, which corresponds to the decrease in the Cr(VI) sorption capacities of AC-CSP from 95.6 to 87.8 mg/g. This indicates that the treated bed volume increases with a higher Empty Bed Residence Time (EBRT). In other words, with higher EBRT, Cr(VI) ion has more time to contact with AC-CSP, which results in higher removal of Cr(VI) ion in the fixed-bed column.

3.3.3. Effect of initial concentrations on the sorption of Cr(VI) by AC-CSP

The effect of influent Cr(VI) concentration on the performance of the breakthrough curve was determined by varying the Cr(VI) concentrations between 200 and 500 mg/L (Fig. 8b). The flow rate, initial influent pH and bed height were maintained at 3.3 ml/min, 5.12 and 2.0 cm, respectively.

As seen in Fig. 8b, for low influent concentration of Cr(VI), the breakthrough occurs late and surface of AC-CSP is saturated with Cr(VI) after a long time whereas for higher Cr(VI) concentration, the breakthrough occurs in a short period of time. This indicates that the binding sites in AC-CSP become more quickly saturated as the Cr(VI) concentration increases. While the sorption capacity of AC-CSP is found to increase from 95.6 to 112.5 mg/g with increase in initial Cr(VI) concentration from 200 to 500 mg/L; this may be due to the higher driving force at high influent Cr(VI) concentration, which will be beneficial to the alleviation of the mass transfer resistance in the transfer process. In addition, the breakthrough curve is slightly sharper at higher influent Cr(VI) concentration, implying a relatively smaller mass transfer zone and intra-particle diffusion in control of the process. The same trend was also observed in the work of Goel et al. [36] and Baral et al. [37], related to lead (II) and Cr(VI) ions sorption, respectively.

3.3.4. Desorption tests

The stability and regeneration potential of AC-CSP was also examined by eluting distilled water and NaCl solution (1 mol/L). The elution of Cr(VI) by distilled water is only 2.5%; this illustrates the insignificance of physical bonding in the sorption of Cr(VI) by AC-CSP. As shown in Fig. 9, the process of sorption–desorption by NaCl solution was repeated for three successive cycles and the biosorbent shows a certain decrease in the sorption capacity during successive cycles. The elution of Cr(VI) ion from AC-CSP by NaCl solution can be interpreted according to the following mechanism:

$$RNH_2{}^+HCrO_4{}^- + NaCl \leftrightarrow RNH_2{}^+Cl^- + HCrO_4{}^- \quad (7)$$

It is observed that the desorption efficiencies during three successive cycles are 75.9%, 69.8% and 64.3%, respectively. The loss of the sorption capacity of AC-CSP may be attributed the binding of residual Cr(VI) with the carboxyl groups, forming the chemical Cr-binding complexes that could not been eluted by NaCl solution.

From the above discussion in desorption tests, it can be concluded that the sorption mechanisms are complicated with ion

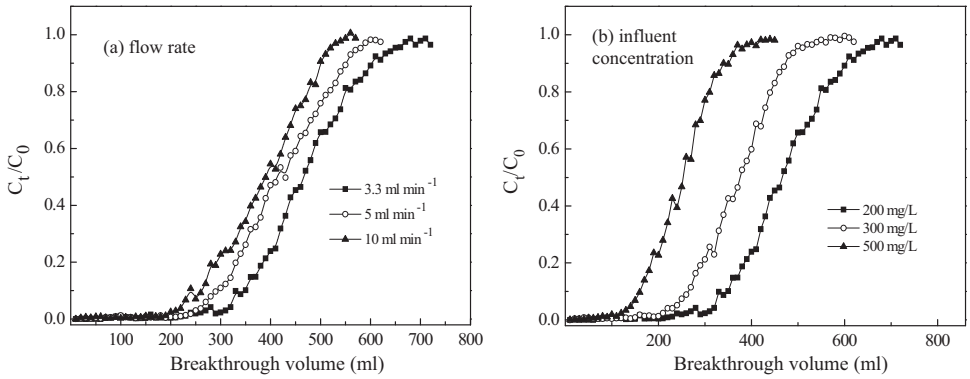

Fig. 8. Effect of flow rate and influent concentration on the breakthrough curves (a, influent Cr(VI) concentration: 200 mg/L, influent pH: 5.12; b, flow rate: 3.3 ml/min, influent pH: 5.12).

exchange and complexation. Similar sorption mechanisms were also reported in the work of Elwakeel for removal of Cr(VI) by chemically modified magnetic chitosan [26].

4. Conclusion

This study investigated the physicochemical and sorption characteristics of the raw CSP and AC-CSP for Cr(VI). The surface characteristics indicated the absence of porous adsorption in the potential Cr(VI) sorption mechanism. Zeta potential and spectrum analysis illustrated a potential relationship between the Cr(VI) sorption mechanisms and the functional groups in AC-CSP. Static, column sorption and desorption tests were conducted, and the sorption capacity of AC-CSP for Cr(VI) was 129.0 mg/g as comparison with 14.8 mg/g of raw CSP. The sorption of Cr(VI) in column was affected by the flow rate and influent Cr(VI) concentration. Higher EBRT resulted in higher removal of Cr(VI) ion in the fixed-bed column. In addition, desorption results of distilled water and NaCl solution (1 mol/L) illustrated the ion exchange and complexation mechanisms for sorption of Cr(VI) by AC-CSP.

Acknowledgments

The research was supported by the National Natural Science Foundation of China (50878121), Key Projects in the National Science & Technology Pillar Program in the Eleventh Five-year Plan Period (2006BAJ08B05-2) and National Major Special Technological Programmes Concerning Water Pollution Control and Management in the Eleventh Five-year Plan Period (2008ZX07010-008-002).

References

[1] V.K. Gupta, A. Rastogi, A. Nayak, Adsorption studies on the removal of hexavalent chromium from aqueous solution using a low cost fertilizer industry waste material, J. Colloid Interface Sci. 342 (2010) 135–141.
[2] K.K. Singh, R. Rastogi, S.H. Hasan, Removal of Cr(VI) from wastewater using rice bran, J. Colloid Interface Sci. 290 (2005) 61–68.
[3] US Department of Health and Human Services, Toxicological Profile for Chromium, Public Health Service Agency for Toxic substances and Diseases Registry, Washington, DC, 1991.
[4] H. Ucuna, Y.K. Bayhana, Y. Kayab, Kinetic and thermodynamic studies of the biosorption of Cr(VI) by *Pinus sylvestris* Linn, J. Hazard. Mater. 153 (2008) 52–59.
[5] G. Moussavi, B. Barikbin, Biosorption of chromium(VI) from industrial wastewater onto pistachio hull waste biomass, Chem. Eng. J. 162 (2010) 893–900.
[6] V.K. Gupta, A. Rastogi, Biosorption of hexavalent chromium by raw and acid-treated green alga *Oedogonium hatei* from aqueous solutions, J. Hazard. Mater. 163 (2009) 396–402.
[7] V. Vinodhini, N. Das, Packed bed column studies on Cr(VI) removal from tannery wastewater by neem sawdust, Desalination 264 (2010) 9–14.
[8] D. Park, Y.S. Yun, J.M. Park, XAS and XPS studies on chromium-binding groups of biomaterial during Cr(VI) biosorption, J. Colloid Interface Sci. 317 (2008) 54–61.
[9] A. Witek-Krowiak, R.G. Szafran, S. Modelski, Biosorption of heavy metals from aqueous solutions onto peanut shell as a low-cost biosorbent, Desalination 265 (2011) 126–134.
[10] A. Bingol, A. Aslan, A. Cakici, Biosorption of chromate anions from aqueous solution by a cationic surfactant-modified lichen (*Cladonia rangiformis* (L.)), J. Hazard. Mater. 161 (2009) 747–752.
[11] C. Namasivayam, M.V. Sureshkumar, Removal of chromium(VI) from water and wastewater using surfactant modified coconut coir pith as a biosorbent, Bioresour. Technol. 99 (2008) 2218–2225.
[12] M. Sekar, V. Sakthi, S. Rengaraj, Kinetics and equilibrium adsorption study of lead(II) onto activated carbon prepared from coconut shell, J. Colloid Interface Sci. 279 (2004) 307–313.
[13] S.S. Baral, S.N. Das, G. Roy Chaudhury, Y.V. Swamy, P. Rath, Adsorption of Cr(VI) using thermally activated weed *Salvinia cucullata*, Chem. Eng. J. 139 (2008) 245–255.
[14] X. Xu, B.Y. Gao, Q.Y. Yue, Q.Q. Zhong, Preparation and utilization of wheat straw bearing amine groups for the sorption of acid and reactive dyes from aqueous solutions, J. Hazard. Mater. 182 (2010) 1–9.
[15] A. Biswas, B.C. Saha, J.W. Lawton, R.L. Shogren, J.L. Willett, Process for obtaining cellulose acetate from agricultural by-products, Carbohydr. Polym. 64 (2006) 134–137.
[16] M.M. Ibrahim, A. Dufresne, W.K. El-Zawawy, F.A. Agblevor, Banana fibers and microfibrils as lignocellulosic reinforcements in polymer composites, Carbohydr. Polym. 81 (2010) 811–819.
[17] U.S. Orlando, A.U. Baes, W. Nishijima, Preparation of agricultural residue anion exchangers and its nitrate maximum adexchange capacity, Chemosphere 48 (2002) 1041–1046.
[18] X. Xu, B.Y. Gao, Q.Y. Yue, Q.Q. Zhong, X. Zhan, Preparation, characterization of wheat residue based anion exchangers and its utilization for the phosphate removal from aqueous solution, Carbohydr. Polym. 82 (2010) 1212–1218.
[19] Y. Wang, B.Y. Gao, W.W. Yue, Q.Y. Yue, Preparation and utilization of wheat straw anionic sorbent for the removal of nitrate from aqueous solution, J. Environ. Sci. 19 (2007) 1305–1310.
[20] R.E. Martinez, O.S. Pokrovsky, J. Schott, E.H. Oelkers, Surface charge and zeta-potential of metabolically active and dead cyanobacteria, J. Colloid Interface Sci. 323 (2008) 317–325.
[21] I.H. Yoon, X.G. Meng, C. Wang, K.W. Kim, S. Bang, E. Choe, L. Lippincott, Perchlorate adsorption and desorption on activated carbon and anion exchange resin, J. Hazard. Mater. 164 (2009) 87–94.
[22] Y. Chen, Y.F. Liu, H.M. Tan, J.X. Jiang, Synthesis and characterization of a novel superabsorbent polymer of N,O-carboxymethyl chitosan graft copolymerized with vinyl monomers, Carbohydr. Polym. 75 (2009) 287–292.
[23] A.M.A. Nada, S. Kamel, M. El-Sakhawy, Thermal behaviour and infrared spectroscopy of cellulose carbamates, Polym. Degrad. Stab. 70 (2000) 347–355.
[24] C.Y. Yin, J.B. Li, Q. Xu, Q. Peng, Y.B. Liu, X.Y. Shen, Chemical modification of cotton cellulose in supercritical carbon dioxide: synthesis and characterization of cellulose carbamate, Carbohydr. Polym. 67 (2007) 147–154.
[25] S.T. Ong, C.K. Lee, Z. Zainal, Removal of basic and reactive dyes using ethylenediamine modified rice hull, Bioresour. Technol. 98 (2007) 2792–2799.
[26] K.Z. Elwakeel, Removal of Cr(VI) from alkaline aqueous solutions using chemically modified magnetic chitosan resins, Desalination 250 (2010) 105–112.
[27] X.S. Wang, L.F. Chen, F.Y. Li, K.L. Chen, W.Y. Wan, Y.J. Tang, Removal of Cr(VI) with wheat-residue derived black carbon: reaction mechanism and adsorption performance, J. Hazard. Mater. 175 (2010) 816–822.
[28] H. Gao, Y.G. Liu, G.M. Zeng, W.H. Xu, T. Li, W.B. Xia, Characterization of Cr(VI) removal from aqueous solutions by a surplus agricultural waste—rice straw, J. Hazard. Mater. 150 (2008) 446–452.
[29] J. Anandkumar, B. Mandal, Removal of Cr(VI) from aqueous solution using Bael fruit (*Aegle marmelos* correa) shell as an adsorbent, J. Hazard. Mater. 168 (2009) 633–640.
[30] D. Park, S.R. Lim, Y.S. Yun, J.M. Park, Development of a new Cr(VI)- biosorbent from agricultural biowaste, Bioresour. Technol. 99 (2008) 8810–8818.
[31] X. Xu, B.Y. Gao, W.Y. Wang, Q.Y. Yue, Y. Wang, S.Q. Ni, Adsorption of phosphate from aqueous solutions onto modified wheat residue: characteristics, kinetic and column studies, Colloids. Surf. B 70 (2009) 46–52.
[32] X.S. Wang, Z.Z. Li, C. Sun, Removal of Cr(VI) from aqueous solutions by low-cost biosorbents: marine macroalgae and agricultural by-products, J. Hazard. Mater. 153 (2008) 1176–1184.
[33] N.K. Hamadi, X.D. Chen, M.M. Farid, M.G.Q. Lu, Adsorption kinetics for the removal of chromium(VI) from aqueous solution by adsorbents derived from used tyres and sawdust, Chem. Eng. J. 84 (2001) 95–105.
[34] T. Karthikeyen, S. Rajgpal, L.R. Miranda, Cr(VI) adsorption from aqueous solution by *Hevea brasilinesis* saw dust activated carbon, J. Hazard. Mater. 124 (2005) 192–199.
[35] A.U. Baes, T. Okuda, W. Nishijima, Adsorption and ion exchange of some groundwater anion contaminants in an amine modified coconut coir, Water Sci. Technol. 35 (1997) 89–95.
[36] J. Goel, K. Kadirvelu, C. Rajgopal, V.K. Garg, Removal of lead(II) by adsorption using treated granular activated carbon batch and column studies, J. Hazard. Mater. 125 (2005) 211–220.
[37] S.S. Baral, N. Das, T.S. Ramulu, S.K. Sahoo, S.N. Das, G. Roy Chaudhury, Removal of Cr(VI) by thermally activated weed *Salvinia cucullata* in a fixed-bed column, J. Hazard. Mater. 161 (2009) 1427–1435.